Available online at www.sciencedirect.com

SciVerse ScienceDirect

Ceramics International 38 (2012) 5973–5978

CERAMICS INTERNATIONAL

www.elsevier.com/locate/ceramint

Highly sensitive H_2S gas sensors based on CuO-coated $ZnSnO_3$ nanorods synthesized by thermal evaporation

Changhyun Jin, Hyunsu Kim, Soyeon An, Chongmu Lee *

Department of Materials Science and Engineering, Inha University, 253 Yonghyun-dong, Incheon 402-751, Republic of Korea

Received 28 December 2011; received in revised form 30 March 2012; accepted 16 April 2012
Available online 23 April 2012

Abstract

$ZnSnO_3$ one-dimensional (1D) nanostrutures were synthesized by thermal evaporation. The morphology, crystal structure and sensing properties of the CuO-coated $ZnSnO_3$ nanostructures to H_2S gas at 100 °C were examined. Transmission electron microscopy and X-ray diffraction revealed both the $ZnSnO_3$ nanorods and CuO nanoparticles to be single crystals. The diameters of the CuO nanoparticles on the nanorods ranged from a few to a few tens of nanometers. The gas sensors fabricated from multiple networked CuO-coated $ZnSnO_3$ nanorods exhibited enhanced electrical responses to H_2S gas compared to the uncoated $ZnSnO_3$ nanorod sensors, showing 61.7-, 49.9-, and 31.3-fold improvement at H_2S concentrations of 25, 50, and 100 ppm, respectively. The response time of the nanorod sensor to H_2S gas was reduced by the CuO coating but the recovery time was similar. The mechanism for the enhanced H_2S gas sensing properties of $ZnSnO_3$ nanorods by the CuO coating is discussed.

Keywords: $ZnSnO_3$; Nanorods; Thermal evaporation; CuO; H_2S

1. Introduction

H_2S is used widely in industry despite being highly toxic and flammable, potentially causing people to lose consciousness at very low concentrations [1]. Therefore, H_2S at concentrations as low as a few tens of ppm should be detected to prevent exposure to H_2S gas. Over the past decades, thin and thick film gas sensors based on a range of metal oxide materials, such as SnO_2, CuO, WO_3, In_2O_3, ZnO and Fe_2O_3, have been studied, but these metal oxides have inherent shortcomings of poor selectivity, long response times, limited detection range, and the requirement of a high operating temperature [2]. To overcome these problems, one-dimensional (1D) nanostructure-based sensors have been studied intensively in recent years. 1D nanostructure sensors offer advantages, such as higher sensitivity, superior spatial resolution and rapid response associated with 1D nanostructures, due to the high surface-to-volume ratios compared to thin film gas sensors [3–7]. Enhancing their sensing performance and detection limit is still a challenge. The sensing properties of metal oxide 1D nanosensors are often improved by the functionalization of metal oxides with catalysts, such as Pd [8], Pt [9], Au [10], Ag [11] and Cu [12] or coating with CuO [13], WO_3 [14], and Fe_2O_3 [15]. Of these materials for functionalization or coating, CuO is particularly effective in improving the hydrogen sulfide (H_2S) gas sensing properties of metal oxide 1D nanosensors.

According to previous reports, the sensitivity of SnO_2 to H_2S was enhanced considerably by doping with a small amount of CuO [15]. The enhanced sensitivity was attributed to n-type SnO_2-p-type CuO heterojunction formation and the strong affinity of CuO–H_2S, which disrupts the p–n junction. Thick films of SnO_2 doped with 5% CuO were reported to exhibit very high sensitivity [16]. On the other hand, the sensor response time was as long as 20 min. CuO–SnO_2 thin films deposited by spray pyrolysis and microwave plasma CVD were also reported to exhibit rapid response and recovery times of a few minutes, and their sensitivity was approximately 10^3 at a H_2S concentration of 50 ppm [17,18]. One report stated that CuO–SnO_2 hybrid thin films synthesized by the simultaneous evaporation of Sn and Cu metals at 133.32 Pa showed a sensitivity of approximately 10^2 to H_2S gas at 10 ppm at 200 °C [19].

Zinc stannate ($ZnSnO_3$) has also attracted considerable attention as a gas sensing material [20–27]. This material has been used to sense reducing and combustible gases, such as

* Corresponding author. Tel.: +82 32 860 7536; fax: +82 32 862 5546.
E-mail address: cmlee@inha.ac.kr (C. Lee).

0272-8842/$36.00
http://dx.doi.org/10.1016/j.ceramint.2012.04.050

liquid petrol gas, ethanol, carbon monoxide, petroleum, formaldehyde and H_2S [20–27]. Recently, a range of $ZnSnO_3$ nanostructures including nanoparticles, nanorods, nanotubes and hollow nanostructures have been synthesized. Owing to its instability at temperatures above 600 °C [28], relatively lower temperature synthesis methods, such as low-temperature ion exchange [29] and coprecipitation methods, have been used to prepare $ZnSnO_3$ nanostructures [30]. Nevertheless, these synthesis strategies usually require complex operating procedures, expensive raw materials, and further heat treatment. On the other hand, the hydrothermal synthesis method [31] requires high temperatures and considerable time. Therefore, a facile, mild and low-cost method for the synthesis of $ZnSnO_3$ nanostructures is needed. This paper reports the synthesis of $ZnSnO_3$ nanorods using a simple thermal evaporation technique as a rapid and facile route in addition to the enhanced sensing properties of $ZnSnO_3$ nanorods coated with CuO in detecting H_2S gas at 100 °C.

2. Experimental

$ZnSnO_3$ nanorods were synthesized using an evaporation technique. Au-coated Si was used as a substrate for the synthesis of the 1D $ZnSnO_3$ structures. The 3 nm Au layer was deposited on a p-type (1 0 0) Si substrate by direct current (dc) sputtering. A quartz tube was mounted horizontally inside a tube furnace. A 1:1:3 mixture of 99.99% pure SnO_2, 99.99% pure ZnO, and graphite powders were placed on the holder in the high temperature zone (1000 °C) whereas an Au-coated Si substrate was placed on the holder in the low temperature zone (700 °C). The thermal evaporation process was carried out for 1 h in an Ar/O_2 atmosphere with constant flow rates of oxygen (O_2) (5 sccm) and Ar (95 sccm). The total pressure was 0.95 Torr.

CuO thin films were deposited on the surfaces of the $ZnSnO_3$ nanorod samples using a wet method. A 5 mM ethanolic $Cu(NO_3)_2$ H_2O solution ($Cu(NO_3)_2$ H_2O:ethanol = 12.08 mg:10 ml) was prepared in a vial. The $ZnSnO_3$ nanorod samples were immersed in the solution and the vial was placed in a home-made ultraviolet (UV) box. Subsequently, the solution and alumina bath were irradiated with 360 nm UV light at 3 mW/cm^2 for 20 min. Finally, the CuO-coated $ZnSnO_3$ nanorod samples were annealed at 600 °C at 0.95 Torr for 30 min in an Ar (95 sccm)/O_2 (5 sccm) atmosphere. The collected nanorod samples were characterized by scanning electron microscopy (SEM, Hitachi S-4200), transmission electron microscopy (TEM, Philips CM-200) equipped with an energy dispersive X-ray spectrometer (EDXS).

The CuO-coated $ZnSnO_3$ nanorods were dispersed ultrasonically in a mixture of deionized water (5 ml) and isopropyl alcohol (5 ml), and dried at 90 °C for 30 min. A 200 nm thick SiO_2 film was grown thermally on single crystalline Si (1 0 0). A slurry droplet containing the $ZnSnO_3$ nanorods (10 μl) was dropped onto the SiO_2-coated Si substrates equipped with a pair of interdigitated (IDE) Ni (~200 nm)/Au (~50 nm) electrodes with a gap of 20 μm. The gas sensing properties of the as-synthesized and CuO-coated $ZnSnO_3$ nanorods were measured at 100 °C in a quartz tube placed in a sealed chamber with an electrical feed through. Pure H_2S (>99.99%) gas was flowed into the testing tube while measuring the electrical resistance of the nanorods. The sensing characteristics of the gas sensors was recorded at different H_2S concentrations (25, 50 and 100 ppm) when a potential difference of 0.5 V was applied between the IDE Ni/Au electrodes. The conventional definition of a response to a reducing gas (i.e. $(R_a - R_g)/R_g$, where R_a and R_g are the electrical resistances of the sensors in air and target gas, respectively) was used to evaluate the responses of the n-type $ZnSnO_3$ nanonod sensors to H_2S. The response time was defined as the time needed for the variation in electrical resistance to reach 90% of the equilibrium value after injecting the gas, and the recovery time was defined as the time needed for the sensor to return to 90% above the original resistance in air after removing the gas.

3. Results and discussion

SEM of the as-synthesized $ZnSnO_3$ 1D nanostructures revealed diameters ranging from 60 to 100 nm with lengths up to a few hundreds of micrometers (Fig. 1a). A typical EDX spectrum (Fig. 1b) taken from a typical CuO-functionalizd $ZnSnO_3$ nanorod (Fig. 1a, inset) exhibited peaks for Zn, Sn and O. The low-magnification TEM image (Fig. 2a) showed that CuO nanoparticles with diameters ranging from a few to a few tens of nanometers were distributed around a $ZnSnO_3$ nanorod.

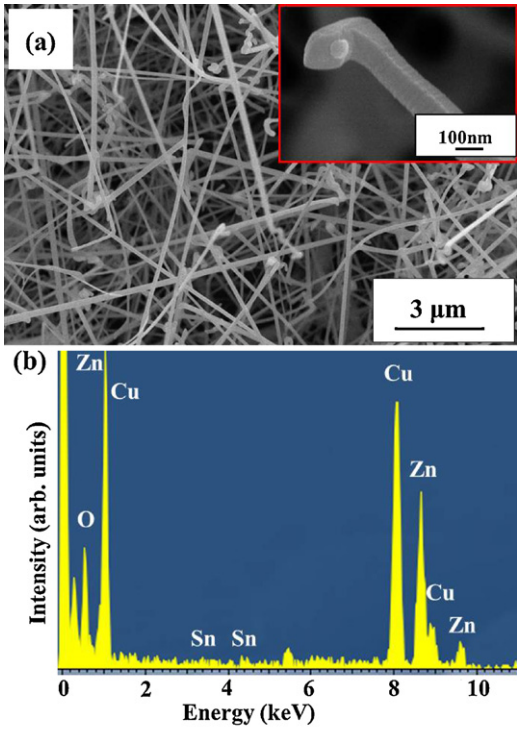

Fig. 1. (a) SEM image of CuO-coated $ZnSnO_3$ nanorods. Inset, enlarged SEM image of a typical CuO-coated $ZnSnO_3$ nanorod. (b) EDX spectrum of CuO-coated $ZnSnO_3$ nanorods.

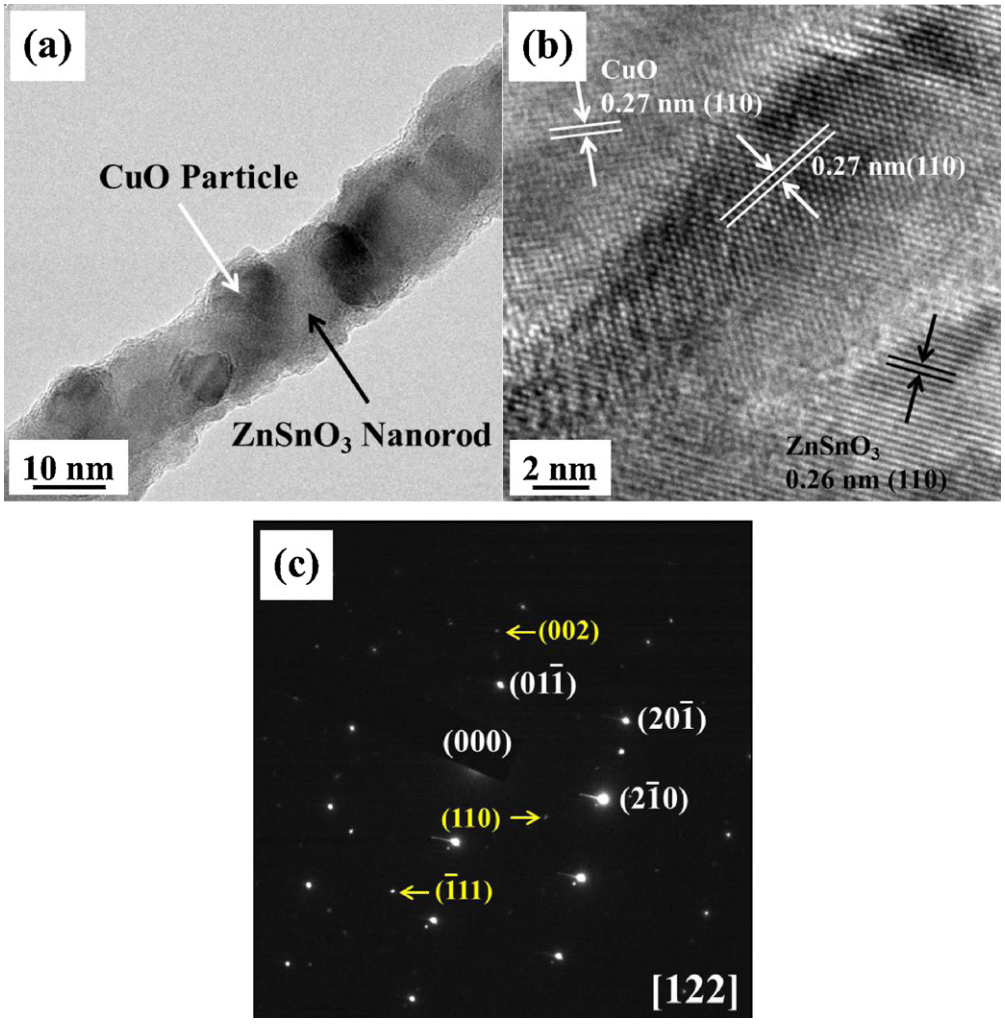

Fig. 2. (a) Low-magnification TEM image of a typical of CuO-coated $ZnSnO_3$ nanorod. (b) Local HRTEM image of the nanostructure at the interface region of a $ZnSnO_3$ nanorod and a CuO nanoparticle. (c) SAED pattern of the [1 2 2] zone axis of the nanomaterial at the same region as in (b).

The HRTEM image (Fig. 2b) exhibited a fringe pattern clearly, indicating that the $ZnSnO_3$ nanorods are single crystals. The resolved distance between the two neighboring parallel fringes in the $ZnSnO_3$ nanorod region was 0.26 nm, which is in good agreement with the interplanar spacing of the (1 1 0) planes in $ZnSnO_3$. The corresponding SAED pattern (Fig. 2c) confirmed that an individual nanorod is a $ZnSnO_3$ single crystal with a rhombohedral structure and lattice constants of $a = 0.5283$ nm and $c = 1.4091$ (JCPDS No. 52-1381). Dim reflection spots from CuO were also observed in the SAED pattern. The dim spotty pattern indicated that CuO has a monocrystalline monoclinic structure with a lattice constant $a = 0.4684$ nm, $b = 0.3425$ nm, $c = 0.5129$ nm, and $\beta = 99.47$ (JCPDS No. 05-0661). The resolved distance between the two neighboring parallel fringes in the CuO nanoparticle region was 0.27 nm, which is in good agreement with the interplanar spacing of the (1 1 0) planes in bulk CuO. Fig. 3 shows the X-ray diffraction (XRD) pattern of the CuO-coated $ZnSnO_3$ nanorods. The main diffraction peaks in the pattern of the as-synthesized nanorods (Fig. 3) were indexed to a rhombohedral-structured single crystal $ZnSnO_3$, indicating that the nanomaterial is $ZnSnO_3$. In addition to the reflections from $ZnSnO_3$, several reflection peaks from CuO were also observed, confirming that the CuO particles are also crystalline.

The H_2S gas sensing properties of both CuO-coated and uncoated $ZnSnO_3$ nanorod sensors were examined at 100 °C. The curves in Fig. 4a and c show the measured resistance as a function of time for the uncoated $ZnSnO_3$ nanorods and

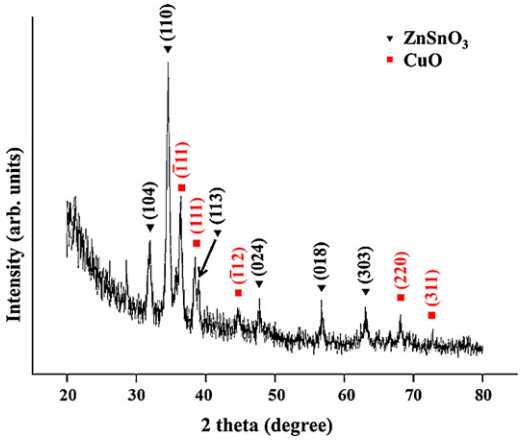

Fig. 3. XRD pattern of the CuO-coated $ZnSnO_3$ nanorods.

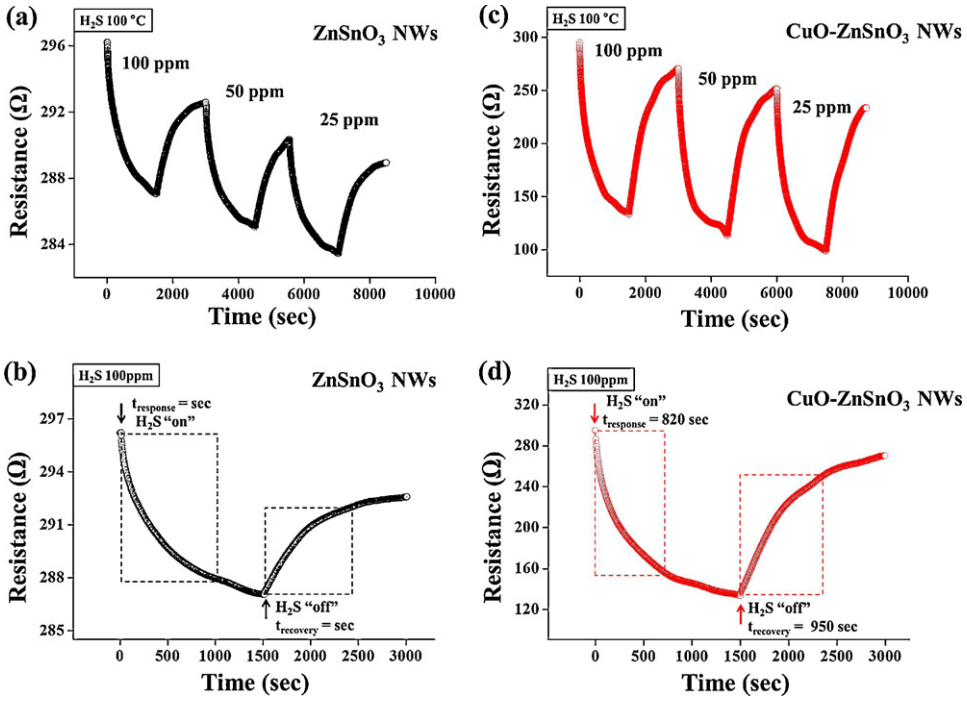

Fig. 4. Electrical responses of the gas sensors to 25, 50 and 100 ppm H_2S gas at 100 °C fabricated from pure and CuO-coated $ZnSnO_3$ nanorods: (a) The dynamic response curve and (b) enlarged part of the response curve to 100 ppm H_2S gas of pure $ZnSnO_3$ nanorods. (c) Dynamic response curve and (d) enlarged part of the response curve to 100 ppm H_2S gas of CuO-coated $ZnSnO_3$ nanorods.

CuO-coated $ZnSnO_3$ nanorods, respectively, exposed to 25, 50 and 100 ppm H_2S. The resistance decreased upon exposure to H_2S and recovered upon the removal of H_2S but the recovered resistance was lower than the initial value. The sensor responses were quite stable and reproducible for repeated testing cycles. Fig. 4b and d, respectively, show the enlarged parts of the data in Fig. 4a and c measured at a H_2S concentration of 100 ppm for both the pure $ZnSnO_3$ nanorods and CuO-coated $ZnSnO_3$ nanorods to reveal the moments of gas input and gas stop. The response to H_2S was enhanced considerably by the CuO coating (Table 1). Uncoated $ZnSnO_3$ nanorods showed responses of 2.47, 2.70 and 3.84% at H_2S concentrations of 25, 50 and 100 ppm, respectively. In contrast, the CuO-coated $ZnSnO_3$ nanorods showed responses of 152.5, 134.8, and 120.2% at H_2S concentrations of 25, 50 and 100 ppm, respectively. Therefore, the responses of the nanorods were improved 61.7-, 49.9-, and 31.3-fold at H_2S concentrations of 25, 50, and 100 ppm, respectively. Also, these response values are approximately 4- to 10-fold higher than those obtained previously from pure $ZnSnO_3$ nanorods by Zeng et al. [25] (Table 2).

The H_2S gas sensing mechanism of the CuO-coated $ZnSnO_3$ nanorods was modeled based on the model proposed for the SnO_2-core/CuO-shell 1D nanostructures [32,33]. $ZnSnO_3$ nanorods have relatively high electrical resistance at low temperatures because $ZnSnO_3$ is a wide bandgap semiconductor ($E_g = 3.7$ eV) [34]. In the case of uncoated $ZnSnO_3$ nanorods, the electrons in the conduction band can be trapped by oxygen species, resulting in an electron depletion layer on the surface of the $ZnSnO_3$ nanorod, which can make the material highly resistive. Upon exposure to H_2S gas, the following reaction occurs spontaneously between H_2S and the preadsorbed oxygen species at 100 °C:

$$H_2S(g) + 3O_2 - (ads) = 2H_2O + 2SO_2(g) + 3e^-$$
$$\Delta G^\circ{}_{373\,K} = -979.3\,kJ/mol \quad (1)$$

The electrons released from the surface states recombine with the holes in the valance band, resulting in a decrease in electrical resistance. In the process of surface sensing, the electrons trapped by surface oxygen species will be fed back into the electron depletion layer, which will decrease the electrical resistance of $ZnSnO_3$.

On the other hand, in the case of CuO-coated $ZnSnO_3$ nanorods, the electrical resistance is very high at the interface of the n-type $ZnSnO_3$ and p-type CuO in air due to the

Table 1
H_2S gas sensing responses of pure and CuO-coated $ZnSnO_3$ nanorods.

H_2S conc. (ppm)	Response (%)		Response time (s)		Recovery time (s)	
	$ZnSnO_3$	CuO–$ZnSnO_3$	$ZnSnO_3$	CuO–$ZnSnO_3$	$ZnSnO_3$	CuO–$ZnSnO_3$
100	3.84	120.15	1080	820	970	950
50	2.70	134.78	870	800	790	990
25	2.47	152.52	990	800	920	890

Table 2
Comparison of H_2S gas sensing responses between present work and previous work.

H_2S conc. (ppm)		5	10	20	25	50	100
Response (%)	$ZnSnO_3$ NWs (present work)	–	–	–	2.5	2.7	3.8
	CuO–$ZnSnO_3$ NWs (present work)	–	–	–	153	135	120
	$ZnSnO_3$ (Ref. [25])	2.7	5.0	8.9	-	17.6	29.4

formation of p–n junctions. Upon exposure to H_2S gas, a CuS layer might form on the surface of the CuO nanorods according to the following spontaneous chemical reaction:

$$\begin{aligned} &CuO(g) + H_2S(s) \rightarrow CuS(s) + H_2O(g) \\ &\Delta G^{\circ}{}_{373\,K} = -121.0\,kJ/mol \end{aligned} \quad (2)$$

The formation of CuS destroys the p–n junction, resulting in a decrease in electrical resistance because CuS is metallic in nature. CuS formation has been observed previously by X-ray photoelectron spectroscopy, XRD, and Raman spectroscopy [32]. Consequently, the resistance of the nanorod sensor is far lower in H_2S gas than in air. When the H_2S gas supply is stopped, the CuS layer formed at the surface of the nanorod will be oxidized in air and converted back to CuO through the following reaction:

$$CuS + 3O_2 \rightarrow 2CuO + 2SO_2 \quad (3)$$

Table 1 shows that the response time of the nanorod sensor for H_2S gas sensing was decreased considerably by the CuO coating but the recovery time was similar. The origin of this decrease in response time is unclear but it might be due to the higher rate of Reaction (2) than Reaction (1).

4. Conclusions

The morphology, crystal structure, and enhanced sensing characteristics of the $ZnSnO_3$ nanostructures coated with CuO to H_2S gas at 100 °C were examined. The $ZnSnO_3$ 1D nanostructures synthesized using an evaporation technique were rod-like with diameters ranging from 60 to 100 nm and lengths up to a few hundreds of micrometers. The diameters of the CuO nanoparticles on the nanorods ranged from a few to a few tens of nanometers. The gas sensors fabricated from multiple-networked, CuO-coated $ZnSnO_3$ nanorods exhibited enhanced electrical responses to H_2S gas at 100 °C. The responses of the nanorods were improved 61.7-, 49.9- and 31.3-fold at H_2S concentrations of 25, 50, and 100 ppm, respectively. The response time of the nanorod sensor for H_2S gas sensing was shortened by the CuO coating, even though the recovery time was not changed. The enhanced electrical response of the CuO-coated $ZnSnO_3$ nanorod sensor to H_2S gas compared to that of the uncoated $ZnSnO_3$ nanorod sensor was attributed to destruction of the p–n junctions due to the formation of metallic CuS.

Acknowledgment

This study was supported financially by theKorean Research Foundation (KRF) through the 2010 Core Research Program.

References

[1] Z. Zeng, K. Wang, Z. Zhang, J. Chen, W. Zhou, The detection of H_2S at room temperature by using individual indium oxide nanowire transistors, Nanotechnology 20 (2009) 045503–045506.
[2] N.S. Ramgir, S.K. Ganapathi, M. Kaur, N. Datta, K.P. Muthe, D.K. Aswal, S.K. Gupta, J.V. Yakhmi, Sub-ppm H_2S sensing at room temperature using CuO thin films, Sensors and Actuators B 151 (2010) 90–96.
[3] >A. Kolmakov, Y. Zhang, G. Cheng, M. Moskovits, Detection of CO and O_2 using tin oxide nanowire sensors, Advanced Materials 15 (2003) 997–1000.
[4] Y. Liu, E. Koep, M. Liu, A highly sensitive and fast-responding SnO_2 sensor fabricated by combustion chemical vapor deposition, Chemistry of Materials 17 (2005) 3997–4000.
[5] M. Law, H. kind, B. Messer, F. Kim, P. Yang, Photochemical sensing of NO_2 with SnO_2 nanoribbon nanosensors at room temperature, Angewandte Chemie 114 (2002) 2511–2514.
[6] Y.H. Lin, M.W. Huang, C.K. Liu, J.R. Chen, J.M. Wu, H.C. Shih, The preparation and high photon-sensing properties of fluorinated tin dioxide nanowires, Journal of the Electrochemical Society 156 (2009) K196–K199.
[7] N.S. Ramgir, I.S. Mulla, K.P. Vijayamohanan, A room temperature nitric oxide sensor actualized from Ru-doped SnO_2 nanowires, Sensors and Actuators B 107 (2005) 708–715.
[8] Y. Wang, F. Kong, B. Zhu, S. Wang, S. Wu, W. Huang, Synthesis and characterization of Pd-doped α-Fe_2O_3 H_2S sensor with low power consumption, Materials Science and Engineering B 140 (2007) 98–102.
[9] Y. Shen, T. Yamazaki, Z. Liu, D. Meng, T. Kikuta, Hydrogen sensors made of undoped and Pt-doped SnO_2 nanowires, Journal of Alloys and Compounds 488 (2009) L21–L25.
[10] S.W. Choi, S.H. Jung, S. Kim, Significant enhancement of the NO_2 sensing capability in networked SnO_2 nanowires by Au nanoparticles synthesized via γ-ray radiolysis, Journal of Hazardous Materials 193 (2011) 243–248.
[11] J. Gong, Q. Chen, M.R. Lian, N.C. Liu, R.G. Stevenson, F. Adami, Micromachined nanocrystalline silver doped SnO_2 H_2S sensor, Sensors and Actuators B – Chemical 114 (2006) 32–39.
[12] M.S. Wagh, L.A. Patil, T. Seth, D.P. Amalnerkar, Surface cupricated SnO_2–ZnO thick films as a H_2S gas sensor, Materials Chemistry and Physics 84 (2004) 228–233.
[13] I.S. Hwang, J.K. Choi, S.J. Kim, K.Y. Dong, J.H. Kwon, B.K. Ju, J.H. Lee, Enhanced H_2S sensing characteristics of SnO_2 nanowires functionalized with CuO, Sensors and Actuators B 142 (2009) 105–110.
[14] C. Zhang, M. Debliquy, A. Boudiba, H. Liao, C. Coddet, Sensing properties of atmospheric plasma-sprayed WO_3 coating for sub-ppm NO_2 detection, Sensors and Actuators B 144 (2010) 280–288.
[15] T. Maekawa, J. Tamaki, N. Miura, N. Yamazoe, Sensing behavior of CuO-loaded SnO_2 element for H_2S detection, Chemistry Letters 20 (1991) 575.
[16] J. Tamaki, T. Maekawa, N. Miura, N. Yamazoe, CuO–SnO_2 element for highly sensitive and selective detection of H_2S, Sensors and Actuators B 9 (1992) 197–203.
[17] D.J. Yoo, J. Tamaki, S.J. Park, N. Miura, N. Yamazoe, Copper oxide-loaded tin dioxide thin film for detection of dilute hydrogen sulfide, Journal of Applied Physics 34 (1995) L455–L457.
[18] S. Manorama, G.S. Devi, V.J. Rao, Hydrogen sulfide sensor based on tin oxide deposited by spray pyrolysis and microwave plasma chemical vapor deposition, Applied Physics Letters 64 (1994) 3163–3165.
[19] J. Tamaki, K. Shimanoe, Y. Yamada, Y. Yamamoto, N. Miura, N. Yamazoe, Dilute hydrogen sulfide sensing properties of CuO–SnO_2 thin

film prepared by low-pressure evaporation method, Sensors and Actuators B 49 (1998) 121–125.
[20] J.Q. Xu, X.H. Jia, X.D. Lou, G.X. Xi, J.J. Han, Q.H. Gao, Selective detection of HCHO gas using mixed oxides of ZnO/$ZnSnO_3$, Sensors and Actuators B 120 (2007) 694–699.
[21] B. Geng, C. Fang, F. Zhan, N. Yu, Synthesis of polyhedral $ZnSnO_3$ microcrystals with controlled exposed facets and their selective gas-sensing properties, Small 4 (2008) 1337–1343.
[22] P. Song, Q. Wang, Z. Yang, Biomorphic synthesis of $ZnSnO_3$ hollow fibers for gas sensing application, Sensors and Actuators B 156 (2011) 983–989.
[23] H. Men, P. Gao, B. Zhou, Y. Chen, C. Zhu, G. Xiao, L. Wang, M. Zhang, Fast synthesis of ultra-thin $ZnSnO_3$ nanorods with high ethanol sensing properties, Chemical Communications 46 (2010) 7581–7583.
[24] Y. Zeng, T. Zhang, H. Fan, G. Lu, M. Kang, Synthesis and gas-sensing properties of $ZnSnO_3$ cubic nanocages and nanoskeletons, Sensors and Actuators B 143 (2009) 449–453.
[25] Y. Zeng, K. Zhang, X. Wang, Y. Sui, B. Zou, W. Zheng, G. Zou, Rapid and selective H_2S detection of hierarchical $ZnSnO_3$ nanocages, Sensors and Actuators B 159 (2011) 245–250.
[26] J. Xu, X. Jia, X. Lou, J. Shen, One-step hydrothermal synthesis and gas sensing property of $ZnSnO_3$ microparticles, Solid State Electronics 50 (2006) 504–507.
[27] Y. Cao, D. Jia, J. Zhou, Y. Sun, Simple solid-state chemical synthesis of $ZnSnO_3$ nanocubes and their application as gas sensors, European Journal of Inorganic Chemistry 2009 (2009) 4105–4109.
[28] Y.S. Shen, T.S. Zhang, Preparation, Structure and gas-sensing properties of ultramicro $ZnSnO_3$ powder, Sensors and Actuators B 12 (1993) 5–9.
[29] X.Y. Xue, Y.J. Chen, Q.H. Li, C. Wang, Y.G. Wang, T.H. Wang, Electronic transport characteristics through individual $ZnSnO_3$ nanowires, Applied Physics Letters 88 (2006) 182102–182103.
[30] D. Kovacheva, K. Petrov, Preparation of crystalline $ZnSnO_3$ from Li_2SnO_3 by low-temperature ion exchange, Solid State Ionics 109 (1998) 327–332.
[31] Y. Zeng, T. Zhang, H.T. Fan, W.Y. Fu, G.Y. Lu, Y.M. Sui, H.B. Yang, One-pot synthesis and gas-sensing properties of hierarchical $ZnSnO_3$ nanocages, Journal of Physical Chemistry C 113 (2009) 19000–19004.
[32] G.S. Devi, S. Manorama, V.J. Rao, High sensitivity and selectivity of an SnO_2 sensor to H_2S at around 100 °C, Sensors and Actuators B 28 (1995) 31–37.
[33] A. Chowdhuri, P. Sharma, V. Gupta, K. Sreenivas, K.V. Rao, H_2S gas sensing mechanism of SnO_2 films with ultrathin CuO dotted islands, Journal of Applied Physics 92 (2002) 2172–2180.
[34] M. Miyauchi, Z. Liu, Z.G. Zhao, S. Anandan, K. Hara, Single crystalline zinc stannate nanoparticles for efficient photo-electrochemical devices, Chemical Communications 46 (2010) 1529–1531.